

# Joint Optimization of UAV Trajectory and Sensor Uploading Powers for UAV-Assisted Data Collection in Wireless Sensor Networks

Yinlu Wang<sup>ID</sup>, *Student Member, IEEE*, Ming Chen, *Member, IEEE*, Cunhua Pan<sup>ID</sup>, *Member, IEEE*, Kezhi Wang<sup>ID</sup>, *Senior Member, IEEE*, and Yijin Pan<sup>ID</sup>, *Member, IEEE*

**Abstract**—In this article, we investigate the energy minimization problem of an unmanned-aerial-vehicle (UAV)-assisted data collection sensor network. We jointly optimize the trajectory of the UAV and the power consumption of the sensors for data uploading with the power and energy constraints of sensors. The trajectory design consists of two parts: 1) the serving orders for sensors and 2) the UAV’s hovering positions, where the latter is highly coupled with the power consumption of the sensors. To find the optimal serving orders of sensors, we formulate the problem as a standard traveling salesman problem (TSP), which can be optimally solved by the efficient Cutting-Plane method. To solve the UAV position and sensor uploading power optimization problem, we propose the PSPSCA algorithm that optimizes the transmit power by the pattern search method, while the UAV’s hovering positions are optimized by the successive-convex-approximation (SCA) method in the inner loop. To deal with the high computational complexity of the PSPSCA algorithm, we analyze the analytical relationship between optimal sensor uploading power and the UAV’s hovering positions, based on which we simplify the optimization problem and propose the AQSCA algorithm as an alternative approach. Simulation results have validated that the proposed algorithm outperforms the existing benchmark schemes.

**Index Terms**—Energy minimization, unmanned aerial vehicle (UAV) data collection, UAV trajectory optimization, wireless sensor networks.

Manuscript received July 9, 2021; revised October 1, 2021; accepted November 2, 2021. Date of publication November 9, 2021; date of current version June 23, 2022. This work was supported in part by the National Natural Science Foundation of China (NSFC) under Grant 61871128 and Grant 62001107; in part by the Fundamental Research on Foreword Leading Technology of Jiangsu Province under Grant BK20192002; and in part by the Basic Research Project of Jiangsu Provincial Department of Science and Technology under Grant BK20190339. (*Corresponding authors*: Yinlu Wang; Ming Chen.)

Yinlu Wang and Yijin Pan are with the National Mobile Communications Research Laboratory, Southeast University, Nanjing 211111, China (e-mail: yinluwang@seu.edu.cn; panyj@seu.edu.cn).

Ming Chen is with the National Mobile Communications Research Laboratory, Southeast University, Nanjing 211111, China, and also with the Purple Mountain Laboratories, Nanjing 211111, China (e-mail: chenming@seu.edu.cn).

Cunhua Pan is with the School of Electronic Engineering and Computer Science, Queen Mary University of London, London E1 4NS, U.K. (e-mail: c.pan@qmul.ac.uk).

Kezhi Wang is with the Department of Computer and Information Science, Northumbria University Newcastle, Newcastle upon Tyne NE7 7YT, U.K. (e-mail: kezhi.wang@northumbria.ac.uk).

Digital Object Identifier 10.1109/JIOT.2021.3126329

## I. INTRODUCTION

IN WIRELESS sensor networks, most sensor devices have limited computing capabilities. Therefore, data collected by the devices need to be transmitted to a processing center for further analysis. In traditional data collection, sensors either directly transmit data to the collector or form multihop routing paths for transmission. However, direct transmission is energy consuming for remote sensors, while for multihop transmission, sensors close to the collector quickly use up their battery power through frequent relaying. In light of this, many works have considered to use a data mule to collect data from sensors for energy consumption reduction [1]–[3]. The data mule may be a car, a robot, etc., that can travel to the vicinity of each sensor to gather data, which significantly shortens the communication distance and saves the transmission energy of each sensor.

Recently, unmanned-aerial-vehicles (UAVs) were proposed to serve as data mules for sensor network data collection. Compared with conventional ground data mules, such as vehicles and robots, UAV’s flying ability enables it to quickly fly to the vicinity of the devices without being blocked by road obstacles [4]. Besides, the UAV-to-ground links enjoy better channel conditions than ground-to-ground links, providing higher data rate and lower communication energy [5]. In addition, the UAVs can be deployed at remote areas, such as mountains or farms where ground traffic is inconvenient [6]. Therefore, it is promising to use the UAVs to collect data from wireless sensor networks. Nevertheless, the UAV trajectory design remains as a challenging problem for energy-efficient data collection.

The trajectory design problem for UAV data collection in sensor networks can be roughly divided into three categories according to the optimization objectives: 1) energy efficiency maximization; 2) throughput/data rate maximization; and 3) latency minimization.

For the first category, in [7], the energy efficiency of the UAV was maximized by jointly optimizing the trajectory and velocity of the UAV. In [8], the maximum energy consumption of all users was minimized by jointly optimizing the trajectory of the UAV, the serving order of the users and transmission power allocation for users. In [9], the energy consumption of the sensors was minimized by optimizing the clustering and topology of sensors and the trajectory of the UAV.

In [10], the weighted sum energy consumption of multiple UAVs and mobile devices (MDs) was minimized by optimizing the UAV trajectory, UAV-MD association, and the transmission power of MDs. In [11], the maximum user energy consumption was minimized by optimizing the time slot allocation for users and the trajectory of the UAV.

For the second one, the minimum data rate of sensors is maximized by optimizing the 3-D trajectory of the UAV in [12]. In [5], the number of sensors that successfully transmit a required amount of data was maximized by jointly optimizing the trajectory of the UAV and the bandwidth allocation for sensors. For downlink transmission, the throughput of all the UAVs was maximized in [13] by optimizing the 3-D trajectories and transmission powers of the UAVs.

For the third one, in [6], the mission completion time was minimized by optimizing the trajectory, height, and velocity of the UAV and the serving order for sensors. In [14], the mission completion time of the UAV was minimized by optimizing the hovering positions and velocity of the UAV and the data rate of sensors. In [15], the longest mission completion time among all the UAVs was minimized by optimizing the trajectories of the UAVs, the UAV-sensor associations, and the transmission time allocation for sensors.

In recent years, there have been a number of works on UAV trajectory or locations design with different objectives for data collection in wireless sensor networks. For example, Baek *et al.* [4] considered the scenario where a UAV is dispatched to collect data from distributed sensors. The authors addressed the optimization problem of UAV trajectory design aiming at maximizing the minimum residual energy of the sensors, under the constraints of data collection and UAV traveling distance limit. In [16], a number of sensor nodes are grouped into clusters, each of which has a data collection point (CP), and the UAV flies over the CPs to collect data from the sensor nodes. The authors proposed a joint optimization algorithm to optimize the locations of the CPs, the associations of the sensor nodes to the CPs, the sequence of uploading, and the trajectory of the UAV, with the aim of minimizing the age of information of the sensor nodes. In [17], under the scenario of one-to-many data collection, the UAV hovering locations were jointly considered with the objective of maximizing the data collection utility, subject to the constraints of the total hovering duration of the UAV. Chen *et al.* [18] jointly optimized the UAV location, sensor grouping, and power control to maximize the sensors' sum rate, and proposed a UAV-assisted data collection protocol and an efficient grouping and power control nonorthogonal multiple access (NOMA) scheme. Chen *et al.* [19] formulated a data collection maximization problem in a one-to-many UAV data collection sensor network, by jointly optimizing the sensors' data transmission rates and the UAV's hovering positions, subject to the energy constraint of the UAV. Hu *et al.* [20] formulated an optimization problem aiming at minimizing the average age of information of all sensor nodes' data, by jointly optimizing the UAV trajectory, each sensor node's energy harvesting time, and the data collection time. In [21], two data collection optimization problems were formulated, either for the UAV to fully or to partially collect data

from the IoT devices. The hovering positions and the sojourn duration were optimized to maximize the total amount of data collected in each tour, under the energy constraint on the UAV. Feng *et al.* [22] formulated two optimization problems, aiming at maximizing the average throughput and minimizing the outage probability, respectively, by jointly optimizing the trajectory of the UAV and the transmit power of the sensor nodes, subject to the flying speed constraints of the UAV and the average power constraints of each sensor node.

Most of the previous works mentioned above that focused on energy efficiency optimization only minimized the energy consumption of sensors but ignored that of the UAV. In fact, the UAVs have limited battery power and hence its energy should also be minimized. In addition, it is necessary to impose a constraint on the energy consumption of each user to make sure that none of the sensors deplete their battery power before the data collection is completed. For a few works that considered the energy consumption of both the UAV and the sensor nodes, they generally adopted a weighted sum of these two energy consumption as the objective, which cannot guarantee the strict energy budget of the sensors. In this article, we formulate a UAV energy consumption minimization problem by jointly optimizing the UAV trajectory and sensor uploading powers, under strict power and energy consumption constraints of the sensors. To the best of our knowledge, little effort has been made on the UAV flying and hovering energy consumption minimization problem for sensor data collection networks subject to the power and energy constraints of the sensor nodes.

We solve the joint UAV trajectory and sensor uploading power optimization problem by using the following method. First, the UAV trajectory design is divided into two parts: 1) the sensors' serving order and 2) the UAV's hovering positions. Second, the UAV's hovering position optimization is jointly considered with the sensors' uploading power optimization, since these two variables are highly coupled. The serving order design problem is formulated as a standard traveling salesman problem (TSP), which can be optimally and efficiently solved by the Cutting-Plane method. On the other hand, the UAV position and sensor uploading power optimization problem is solved by two algorithms, namely, the optimal PSPSCA algorithm and the near-optimal AQSCA algorithm. In the PSPSCA algorithm, the transmit power vector is optimized by the pattern search method in the outer loop, with the UAV's hovering positions optimized by the successive-convex-approximation (SCA) method in the inner loop. However, the PSPSCA algorithm requires high computational complexity. In light of this, further analysis is made to reveal the analytical relationship between optimal sensor uploading power and the UAV's hovering positions. Based on analytical results, the UAV position and sensor uploading power optimization problem is simplified into a pure UAV trajectory optimization problem, and the AQSCA algorithm is proposed to solve it efficiently. Finally, the optimal solution to the original problem is obtained by iteratively solving the serving order design problem and the joint hovering position and uploading power optimization problem. Simulation results show that

our proposed iterative algorithm outperforms other benchmark schemes.

The contributions of this article are summarized as follows.

- 1) The UAV flying and hovering energy consumption minimization problem is formulated subject to the power and energy constraints of the sensor nodes, which guarantees the power and energy budget of the sensors.
- 2) The JAPQ algorithm is proposed to alternately optimize the serving order of sensors, and the UAV trajectory and sensor uploading power. The sensor serving order optimization problem is formulated as a TSP which is optimally solved by the Cutting-Plane algorithm. The PSPSCA algorithm is proposed to solve the UAV trajectory and sensor uploading power optimization problem. To reduce computational complexity, further analysis is made to reveal the analytical relationship between optimal sensor uploading power and the UAV's hovering positions, based on which the low-complexity AQSCA algorithm is proposed.
- 3) Simulation results have validated the efficiency of the proposed algorithm under various scenarios and its superiority over other benchmark schemes.

The remainder of this article is organized as follows. In Section II, we describe the system model for UAV-assisted data collection in sensor networks and formulate the UAV energy minimization problem. In Section III, we formulate the serving order optimization subproblem as a TSP problem and introduced the Cutting-Plane method to solve it. In Section IV, we present the PSPSCA algorithm and the simplified AQSCA algorithm for solving the joint hovering positions and uploading power optimization subproblem. In Section V, we present extensive simulation results to discuss the performance of the proposed algorithm. Finally, this article is concluded in Section VI.

## II. SYSTEM MODEL AND PROBLEM FORMULATION

Consider a sensor network with  $N$  sensors distributed in a given area. All the sensors collect data from the environment and save the data in its internal storage. Since the sensors' storage capacity is limited, the data will be uploaded to a central processing unit periodically. Suppose a UAV is employed to collect data from the sensors by flying over the sensors along a trajectory. The start and endpoints of the trajectory are predetermined, which could be identical or different. Suppose there are  $N$  hovering points on the trajectory, and at each hovering point the UAV will collect the data from one sensor.

Suppose the UAV flies at a fixed altitude  $H$ . Denote the 2-D coordinate of the  $n$ th sensor as  $\mathbf{w}_n = [x_n, y_n]^T$ ,  $n \in \mathcal{N}$ , where  $\mathcal{N} = \{1, \dots, N\}$  is the set of the sequence numbers of all the sensors. Denote the coordinate of the  $t$ th hovering points of the UAV as  $\mathbf{q}_t = [X_t, Y_t]^T$ ,  $t \in \mathcal{T} \cup \{0, N+1\}$ , where  $\mathcal{T} = \{1, \dots, N\}$  is the set of the sequence numbers of all the hovering points except the start and endpoints. Let the start point be  $\mathbf{q}_0$  and the endpoint be  $\mathbf{q}_{N+1}$ . Denote the trajectory matrix as  $\mathbf{Q} = (\mathbf{q}_1, \dots, \mathbf{q}_N)$ .

Define the association matrix between the hovering points and sensors as  $\mathbf{A} = (a_{nt})_{N \times N}$ , where  $a_{nt} = 1$  if the  $n$ th sensor

uploads its data when the UAV is at the  $t$ th hovering point, and  $a_{nt} = 0$  otherwise. Since at each hovering point the UAV must choose one and only one sensor to collect data from, we have

$$\sum_{t=1}^N a_{nt} = 1 \quad \forall n \in \mathcal{N}$$

$$\sum_{n=1}^N a_{nt} = 1 \quad \forall t \in \mathcal{T}.$$

At the  $t$ th hovering point, the distance between the UAV and the  $n$ th sensor is

$$d_{nt}(\mathbf{q}_t) = \sqrt{\|\mathbf{q}_t - \mathbf{w}_n\|_2^2 + H^2} \quad \forall n \in \mathcal{N} \quad \forall t \in \mathcal{T}. \quad (1)$$

We adopt the following channel pathloss expression:

$$P_r = P_t \beta_0 d^{-2} \quad (2)$$

where  $P_t$  and  $P_r$  are the transmit and receive powers, respectively,  $d$  is the distance between the transmitter and the receiver and, and  $\beta_0$  is the channel power gain at unit distance. Define the channel power gain between the transmitter and the receiver as  $h = P_r/P_t$ , then according to (2) we have  $h = \beta_0 d^{-2}$ . Denote the channel power gain from the  $n$ th sensor to the UAV at the  $t$ th hovering point as  $h_{nt}$ , then we have

$$h_{nt}(\mathbf{q}_t) = \frac{\beta_0}{d_{nt}^2} = \frac{\beta_0}{\|\mathbf{q}_t - \mathbf{w}_n\|_2^2 + H^2}. \quad (3)$$

If the  $n$ th sensor uploads its data when the UAV is at the  $t$ th hovering point, its achievable data rate can be calculated as

$$r_{nt}(p_n, \mathbf{q}_t) = B \log_2 \left( 1 + \frac{p_n h_{nt}}{\sigma^2} \right)$$

$$= B \log_2 \left( 1 + \frac{p_n \beta_0}{\sigma^2 (\|\mathbf{q}_t - \mathbf{w}_n\|_2^2 + H^2)} \right) \quad (4)$$

where  $B$  is the bandwidth,  $\sigma^2$  is the additive Gaussian white noise (AWGN) power,  $p_n$  is the transmit power of the  $n$ th sensor and is constrained by

$$0 \leq p_n \leq P^{\max}. \quad (5)$$

Denote the transmit power vector of all sensors as  $\mathbf{P} = (p_1, \dots, p_N)$ .

Denote the data uploading time from the  $n$ th sensor to the UAV at the  $t$ th hovering point as  $T_{nt}$ , then it can be given by

$$T_{nt}(p_n, \mathbf{q}_t) = \frac{D}{r_{nt}(p_n, \mathbf{q}_t)} \quad \forall n \in \mathcal{N}, t \in \mathcal{T} \quad (6)$$

where  $D$  is the amount of data needs to be uploaded from each sensor to the UAV. Without loss of generality, we assume that all the sensors have the same amount of data, which can be readily generalized to the case when different sensors upload different amount of data. Denote  $\mathbf{a}_n = [a_{n1}, \dots, a_{nN}]^T$ , the energy consumption of the  $n$ th sensor can be given by

$$E_n(\mathbf{a}_n, p_n, \mathbf{Q}) = \sum_{t=1}^N a_{nt} p_n T_{nt}(p_n, \mathbf{q}_t) \quad (7)$$

which should not exceed a given energy consumption threshold  $E_0$ , that is

$$\sum_{t=1}^N a_{nt} p_n T_{nt}(p_n, \mathbf{q}_t) \leq E_0. \quad (8)$$

Denote the hovering/flying energy and power consumption of the UAV as  $E^H$ ,  $E^F$  and  $P^H$ ,  $P^F$ , respectively, then they have the following relationships:

$$E^H(\mathbf{A}, \mathbf{P}, \mathbf{Q}) = P^H \sum_{t=1}^N \sum_{n=1}^N a_{nt} T_{nt}(p_n, \mathbf{q}_t) \quad (9)$$

$$E^F(\mathbf{Q}) = \frac{P^F}{V} \sum_{t=0}^N \|\mathbf{q}_{t+1} - \mathbf{q}_t\|_2 \quad (10)$$

where  $V$  is the UAV flying speed. Thus, the overall energy consumption of the UAV can be given by

$$E^{\text{UAV}}(\mathbf{A}, \mathbf{P}, \mathbf{Q}) = E^H(\mathbf{A}, \mathbf{P}, \mathbf{Q}) + E^F(\mathbf{Q}). \quad (11)$$

The problem that designs the UAV flying trajectory and sensors' uploading power with the aim of minimizing the overall energy consumption of the UAV can be formulated as follows:

$$\begin{aligned} \min_{\mathbf{A}, \mathbf{Q}, \mathbf{P}} & E^{\text{UAV}}(\mathbf{A}, \mathbf{P}, \mathbf{Q}) \\ \text{s.t.} & \end{aligned} \quad (12a)$$

$$C1 : a_{nt} \in \{0, 1\} \quad \forall n \in \mathcal{N}, t \in \mathcal{T} \quad (12b)$$

$$C2 : \sum_{t=1}^N a_{nt} = 1 \quad \forall n \in \mathcal{N} \quad (12c)$$

$$C3 : \sum_{n=1}^N a_{nt} = 1 \quad \forall t \in \mathcal{T} \quad (12d)$$

$$C4 : 0 \leq p_n \leq P^{\max} \quad \forall n \in \mathcal{N} \quad (12e)$$

$$C5 : \sum_{t=1}^N a_{nt} p_n T_{nt}(p_n, \mathbf{q}_t) \leq E_0 \quad \forall n \in \mathcal{N}. \quad (12f)$$

In the above problem, the optimization of matrix  $\mathbf{A}$  determines the serving order for sensors. Given  $\mathbf{A}$ , the decision of  $\mathbf{Q}, \mathbf{P}$  modifies the trajectory by balancing between the flying distance and the data uploading time. We solve Problem (12) by alternately computing the serving order matrix  $\mathbf{A}$ , and the hovering position  $\mathbf{Q}$  and transmit power vectors  $\mathbf{P}$ . This iterative algorithm for jointly solving  $\mathbf{A}$ ,  $\mathbf{Q}$ , and  $\mathbf{P}$  is named as the JAPQ algorithm. The overall solution framework for the JAPQ algorithm is summarized in the following algorithm.

### III. SERVING ORDER OPTIMIZATION

The optimization of the serving order matrix  $\mathbf{A}$  is independent of sensors' transmit power vector  $\mathbf{P}$  but related to the hovering position matrix  $\mathbf{Q}$ . With given  $\mathbf{Q}$ , the optimization problem for  $\mathbf{A}$  reduces to finding the shortest path that passes through each hovering point, which is equivalent to finding the shortest path of the graph shown in Fig. 1.

The graph includes  $N^2 + 2$  vertexes, where the first and the last vertexes stand for the start and endpoints of the UAV. The graph has  $N$  layers, the  $t$ th layer corresponds to the  $t$ th

**Algorithm 1** Framework for the JAPQ Algorithm That Jointly Optimizes  $\mathbf{A}, \mathbf{P}, \mathbf{Q}$

---

Initialize  $\mathbf{P}^{[0]}$  and  $\mathbf{Q}^{[0]}$ .  
**repeat**  
    Given  $\mathbf{P}^{[i]}$  and  $\mathbf{Q}^{[i]}$ , compute the optimal  $\mathbf{A}^{[i]}$  in Sec. III.  
    Given  $\mathbf{A}^{[i]}$ , compute the optimal  $\mathbf{Q}^{[i+1]}$  and  $\mathbf{P}^{[i+1]}$  in Sec. IV.  
    Update  $i = i + 1$ .  
**until**  $\mathbf{A}, \mathbf{P}, \mathbf{Q}$  converge  
Output the optimization result  $\mathbf{A}^*, \mathbf{P}^*, \mathbf{Q}^*$ .

---

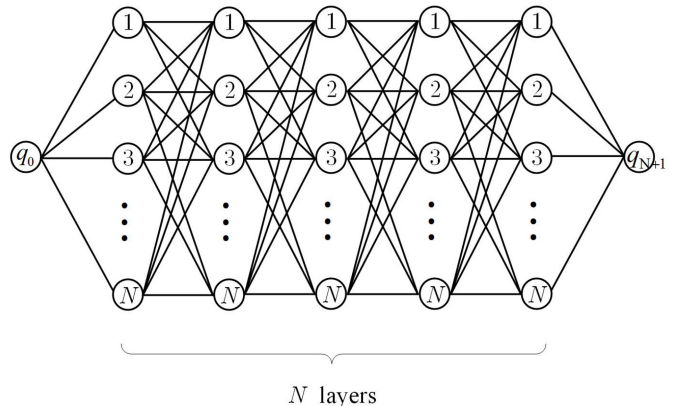


Fig. 1. Graph of the  $\mathbf{A}$  optimization.

hovering point; in each layer, there are  $N$  vertices, where the  $n$ th vertex corresponds to the  $n$ th sensor node. Each path that starts from vertex  $q_0$ , go through one nonrepetitive vertex in each layer, and ends at vertex  $q_{N+1}$ , corresponds to a flight trajectory of the UAV. The weight of each edge stands for the distance between the two hovering points that are represented by the two vertexes of the edge.

Define  $x_{mn}^{(k)}$  as the edge-selecting indicator variable in the  $k$ th step. If  $x_{mn}^{(k)} = 1$ , then the edge  $(m, n)$  is selected in the  $k$ th step; otherwise, the edge  $(m, n)$  is not chosen. Set  $m = 0$  when  $k = 1$  and  $n = 0$  when  $k = N + 1$ . Define  $\mathbf{X}^{(1)} = (x_{0n}^{(1)})_{1 \times N}$ ,  $\mathbf{X}^{(N+1)} = (x_{m0}^{(N+1)})_{1 \times N}$ ,  $\mathbf{X}^{(k)} = (x_{mn}^{(k)})_{N \times N}$  for all  $2 \leq k \leq N$ , and  $\mathbf{X} = (\mathbf{X}^{(1)}, \mathbf{X}^{(2)}, \dots, \mathbf{X}^{(N)}, \mathbf{X}^{(N+1)})$ . Define  $w_{mn}$  as the distance between the  $m$ th hovering point and the  $n$ th hovering point, which is given by

$$w_{mn} = \|\mathbf{q}_m - \mathbf{q}_n\|_2, \quad 0 \leq m \leq N, 1 \leq n \leq N + 1. \quad (13)$$

Then, the shortest path problem is formulated as follows:

$$\begin{aligned} \min_{\mathbf{X}} & \sum_{n=1}^N w_{0n} x_{0n}^{(1)} + \sum_{k=2}^N \sum_{m=1}^N \sum_{n=1}^N w_{mn} x_{mn}^{(k)} \\ & + \sum_{m=1}^N w_{m0} x_{m0}^{(N+1)} \end{aligned} \quad (14a)$$

$$\begin{aligned} \text{s.t.} & \\ & x_{0n}^{(1)}, x_{m0}^{(N+1)}, x_{mn}^{(k)} \in \{0, 1\} \\ & m, n = 1, \dots, N, k = 2, \dots, N \end{aligned} \quad (14b)$$

$$\sum_{m=1}^N \sum_{n=1}^N x_{mn}^{(k)} = 1, k = 2, \dots, N \quad (14c)$$

$$\sum_{n=1}^N x_{0n}^{(1)} = 1 \quad (14d)$$

$$\sum_{m=1}^N x_{m0}^{(N+1)} = 1 \quad (14e)$$

$$\sum_{m=1}^N x_{mn}^{(k)} = \sum_{p=1}^N x_{np}^{(k+1)} \\ n = 1, \dots, N, k = 2, \dots, N \quad (14f)$$

$$x_{0n}^{(1)} = \sum_{p=1}^N x_{np}^{(2)}, n = 1, \dots, N \quad (14g)$$

$$\sum_{m=1}^N x_{mn}^{(N)} = x_{n0}^{(N+1)}, n = 1, \dots, N \quad (14h)$$

$$\sum_{k=2}^{N+1} \sum_{n=1}^N x_{mn}^{(k)} \leq 1, m = 1, \dots, N. \quad (14i)$$

In the above problem, the objective function is the distance of the path, constraint (14b) restricts that the value of the path selection variable should be 0 or 1, constraints (14c)–(14e) restrict one path for each step, (14f)–(14h) specify that the path is continuous, and (14i) restricts that each hovering point should be passed by only once.

The above problem is a standard TSP when the start and endpoints are identical. When the start and endpoints are different, however, it can also be transformed into a standard TSP by adding a dummy point, whose distance to the start and endpoints are set to 0, and that to the sensor nodes are set to be infinite.

Note that for ease of presentation, the formulation in this section slightly differs from the standard representation of the TSP problem. For the standard presentation of the TSP problem, the readers are referred to [23]. The TSP problem is one of the most famous NP-hard problem, which does not have an exponential time exact solution method. Fortunately, for small to moderate TSP problems (typically with node number under 1000), it can be efficiently and optimally solved by the Cutting-Plane method with very little computational time. In this article, we adopt the Cutting-Plane method to optimally solve the  $\mathbf{A}$  optimization problem.

#### IV. JOINT OPTIMIZATION OF HOVERING POSITIONS AND TRANSMISSION POWER

Given  $\mathbf{A}$ , the serving order of each sensor is determined. Denote the serving sequence of the sensors as  $[n_1, n_2, \dots, n_N]$ , which is a permutation of  $[1, \dots, N]$ . Then, Problem (12) reduces to

$$\min_{\mathbf{P}, \mathbf{Q}} \frac{P^F}{V} \sum_{t=0}^N \|\mathbf{q}_{t+1} - \mathbf{q}_t\|_2 + \frac{P^H D}{B} \\ \times \sum_{t=1}^N \log_2^{-1} \left( 1 + \frac{p_{n_t} \beta_0}{\sigma^2 (\|\mathbf{q}_t - \mathbf{w}_{n_t}\|_2^2 + H^2)} \right) \quad (15a)$$

$$\text{s.t. } 0 \leq p_n \leq P^{\max} \quad \forall n \in \mathcal{N} \quad (15b)$$

$$\|\mathbf{q}_t - \mathbf{w}_{n_t}\|_2^2 \leq \tilde{l}(p_{n_t}) \quad \forall t \in \mathcal{N} \quad (15c)$$

where  $\tilde{l}(p_{n_t})$  is a function of  $p_{n_t}$  whose expression is given by

$$\tilde{l}(p_{n_t}) = \frac{p_{n_t} \beta_0}{\sigma^2 \left( 2^{\frac{p_{n_t} D}{E_0 B}} - 1 \right)} - H^2. \quad (16)$$

It can be verified that  $\tilde{l}(p)$  decreases with  $p$ , combining this observation with (15c), we have

$$p_{n_t} \leq p^{(1)} \quad (17)$$

where  $p^{(1)}$  is the unique solution of

$$\tilde{l}(p) = 0. \quad (18)$$

Define  $\tilde{P}^{\max} \triangleq \min\{p^{(1)}, P^{\max}\}$ , then Problem (15) can be rewritten as

$$\min_{\mathbf{P}, \mathbf{Q}} \frac{P^F}{V} \sum_{t=0}^N \|\mathbf{q}_{t+1} - \mathbf{q}_t\|_2 + \frac{P^H D}{B} \\ \times \sum_{t=1}^N \log_2^{-1} \left( 1 + \frac{p_{n_t} \beta_0}{\sigma^2 (\|\mathbf{q}_t - \mathbf{w}_{n_t}\|_2^2 + H^2)} \right) \quad (19a)$$

$$\text{s.t. } 0 \leq p_n \leq \tilde{P}^{\max} \quad \forall n \in \mathcal{N} \quad (19b)$$

$$\|\mathbf{q}_t - \mathbf{w}_{n_t}\|_2 \leq l(p_{n_t}) \quad \forall t \in \mathcal{N} \quad (19c)$$

where

$$l(p_{n_t}) = \sqrt{\tilde{l}(p_{n_t})} = \sqrt{\frac{p_{n_t} \beta_0}{\sigma^2 \left( 2^{\frac{p_{n_t} D}{E_0 B}} - 1 \right)} - H^2}. \quad (20)$$

The joint  $\mathbf{P}, \mathbf{Q}$  optimization problem (19) is still difficult to solve directly due to the highly coupled variables and complicated expressions of the objective function and constraints. In the following section, we propose the PSPSCA algorithm to optimally solve Problem (19) by pattern search of  $\mathbf{P}$  in the outer loop and successively approximating  $\mathbf{Q}$  in the inner loop.

#### A. PSPSCA Algorithm

Given the transmission power vector  $\mathbf{P}^{(r)}$ , Problem (19) reduces to the optimization problem of  $\mathbf{Q}$  as follows:

$$\min_{\mathbf{Q}} \frac{P^F}{V} \sum_{t=0}^N \|\mathbf{q}_{t+1} - \mathbf{q}_t\|_2 + \frac{P^H D}{B} \\ \times \sum_{t=1}^N \left[ \log_2 \left( 1 + \frac{p_{n_t}^{(r)} \beta_0}{\sigma^2 (\|\mathbf{q}_t - \mathbf{w}_{n_t}\|_2^2 + H^2)} \right) \right]^{-1} \quad (21a)$$

$$\text{s.t. } 0 \leq \|\mathbf{q}_t - \mathbf{w}_{n_t}\|_2 \leq l(p_{n_t}^{(r)}) \quad \forall t \in \mathcal{N}. \quad (21b)$$

We solve the above problem by using the SCA method as follows [24].

By introducing auxiliary variable  $\xi$ , and denoting

$$f_{n_t}(\mathbf{q}_t) = \log_2^{-1} \left( 1 + \frac{p_{n_t}^{(r)} \beta_0}{\sigma^2 (\|\mathbf{q}_t - \mathbf{w}_{n_t}\|_2^2 + H^2)} \right).$$

**Algorithm 2** PSPSCA Algorithm for Optimizing  $\mathbf{P}, \mathbf{Q}$ 

- 1: Initialize  $\mathbf{P}^{(0)}$ .
- 2: Using the pattern search method to find an optimal  $\mathbf{P}$  that leads to the minimum objective function value. For each searched  $\mathbf{P}^{(r)}$ , the objective function value is given by running steps 3 to step 6.
- 3: Initialize  $\mathbf{Q}^{[0]}$ .
- 4: **repeat**
- 5:   Substitute  $\mathbf{Q}^{[k]}$  into Problem (25), solve it by using the CVX toolbox and update  $\mathbf{Q}^{[k+1]}$ .
- 6: **until**  $\mathbf{Q}^{[k]}$  converges
- 7: Output the optimization result:  $\mathbf{P}^*, \mathbf{Q}^*$ .

Problem (21) can be transformed into

$$\min_{\mathbf{Q}, \xi} \xi \quad (22a)$$

$$\text{s.t. } \frac{P^F}{V} \sum_{t=0}^N \|\mathbf{q}_{t+1} - \mathbf{q}_t\|_2 + \frac{P^H D}{B} \sum_{t=1}^N f_{n_t}(\mathbf{q}_t) \\ - \xi \leq 0 \quad (22b)$$

$$0 \leq \|\mathbf{q}_t - \mathbf{w}_{n_t}\|_2 \leq l(p_{n_t}^{(r)}) \quad \forall t \in \mathcal{N}. \quad (22c)$$

Let  $\tilde{f}(x) = 1/\log_2(1 + [a/x + b])$ , it is readily to prove that  $\tilde{f}(x)$  is a concave function, so  $f_{n_t}(\mathbf{q}_t)$  is a concave function with respect to  $\|\mathbf{q}_t - \mathbf{w}_{n_t}\|_2^2$ .

Note that the first-order Taylor expansion of a concave function is its global overestimator, so we have

$$\tilde{f}(x) \leq \tilde{f}(x_0) + \tilde{f}'(x_0)(x - x_0) \triangleq f(x_0, x). \quad (23)$$

Let  $a = p_{n_t}^* \beta_0 / \sigma^2$ ,  $b = H^2$ ,  $x = \|\mathbf{q}_t - \mathbf{w}_{n_t}\|_2^2$ ,  $x_0 = \|\mathbf{q}_t^{[k]} - \mathbf{w}_{n_t}\|_2^2$ , we have

$$f_{n_t}(\mathbf{q}_t) \leq \tilde{f}\left(\|\mathbf{q}_t^{[k]} - \mathbf{w}_{n_t}\|_2^2, \|\mathbf{q}_t - \mathbf{w}_{n_t}\|_2^2\right) \triangleq \tilde{f}\left(\mathbf{q}_t^{[k]}, \mathbf{q}_t\right). \quad (24)$$

Initialize  $\mathbf{Q}^{[0]} = (\mathbf{w}_{n_1}, \dots, \mathbf{w}_{n_N})$ , and denote  $\mathbf{Q}^{[k]} = (\mathbf{q}_1^{[k]}, \dots, \mathbf{q}_N^{[k]})$  as the optimized trajectory vector in the  $k$ th iteration, we can solve the following problem to obtain  $\mathbf{Q}^{[k+1]}$ :

$$\min_{\mathbf{Q}, \xi} \xi \quad (25a)$$

$$\text{s.t. } \frac{P^F}{V} \sum_{t=0}^N \|\mathbf{q}_{t+1} - \mathbf{q}_t\|_2 - \xi \\ + \frac{P^H D}{B} \sum_{t=1}^N \tilde{f}(\mathbf{q}_t^{[k]}, \mathbf{q}_t) \leq 0 \quad (25b)$$

$$0 \leq \|\mathbf{q}_t - \mathbf{w}_{n_t}\|_2 \leq l(p_{n_t}^{(r)}) \quad \forall t \in \mathcal{N}. \quad (25c)$$

Problem (25) is a convex optimization problem that can be efficiently solved by the CVX toolbox.

The minimum objective function value under each  $\mathbf{P}^{(r)}$  can be computed by solving Problem (21). To find the optimal  $\mathbf{P}$ , the pattern search method is adopted. The above procedure of jointly optimizing  $\mathbf{P}, \mathbf{Q}$  to solve Problem (19) is named as the “PSPSCA algorithm.” The detailed procedure of this algorithm is summarized in Algorithm 2.

Although the PSPSCA algorithm provides the optimal solution to Problem (19), the pattern search method requires high computational complexity with even a moderate number of sensors. Therefore, in the next section, we propose an approximated AQSCA algorithm that achieves nearly optimal solution with much reduced computational complexity.

**B. AQSCA Algorithm**

To find a low-complexity alternative optimization method for solving Problem (19), we first need to analyze the analytical relationship between the two variable vectors  $\mathbf{P}$  and  $\mathbf{Q}$ . We prove in the following lemma the relationship between the optimal  $\mathbf{P}$  and  $\mathbf{Q}$ .

*Lemma 1:* The optimal solution  $(p_1^*, \dots, p_N^*; \mathbf{q}_1^*, \dots, \mathbf{q}_N^*)$  of Problem (19) satisfies

$$\begin{cases} p_n^* = \tilde{P}^{\max}, & \text{if } \|\mathbf{q}_{t_n}^* - \mathbf{w}_n\|_2 < l(\tilde{P}^{\max}) \\ l(p_n^*) = \|\mathbf{q}_{t_n}^* - \mathbf{w}_n\|_2, & \text{if } l(\tilde{P}^{\max}) \leq \|\mathbf{q}_{t_n}^* - \mathbf{w}_n\|_2 \leq l(0). \end{cases} \quad (26)$$

*Proof:* Define the objective function of Problem (19) as  $L(p_1, \dots, p_N; \mathbf{q}_1, \dots, \mathbf{q}_N)$ , then the Lagrangian function is formulated as

$$\begin{aligned} \mathcal{L}(p_1, \dots, p_N; \mathbf{q}_1, \dots, \mathbf{q}_N) \\ = L(p_1, \dots, p_N; \mathbf{q}_1, \dots, \mathbf{q}_N) + \sum_{n=1}^N \lambda_n(p_n - \tilde{P}^{\max}) \\ + \sum_{n=1}^N \mu_n(-p_n) + \sum_{t=1}^N \xi_t(\|\mathbf{q}_t - \mathbf{w}_{n_t}\|_2 - l(p_{n_t})). \end{aligned} \quad (27)$$

According to the KKT conditions, the optimal solution  $(p_1^*, \dots, p_N^*; \mathbf{q}_1^*, \dots, \mathbf{q}_N^*)$  of Problem (19) must satisfy the following equations:

$$\frac{\partial \mathcal{L}(p_1^*, \dots, p_N^*; \mathbf{q}_1^*, \dots, \mathbf{q}_N^*)}{\partial p_n^*} = 0 \quad \forall n \in \mathcal{N} \quad (28a)$$

$$\frac{\partial \mathcal{L}(p_1^*, \dots, p_N^*; \mathbf{q}_1^*, \dots, \mathbf{q}_N^*)}{\partial \mathbf{q}_t^*} = \mathbf{0} \quad \forall t \in \mathcal{T} \quad (28b)$$

$$\lambda_n(p_n^* - \tilde{P}^{\max}) = 0 \quad \forall n \in \mathcal{N} \quad (28c)$$

$$\mu_n p_n^* = 0 \quad \forall n \in \mathcal{N} \quad (28d)$$

$$\xi_t(\|\mathbf{q}_t^* - \mathbf{w}_{n_t}\|_2 - l(p_{n_t}^*)) = 0 \quad \forall t \in \mathcal{T} \quad (28e)$$

$$0 \leq p_n^* \leq \tilde{P}^{\max} \quad \forall n \in \mathcal{N} \quad (28f)$$

$$\|\mathbf{q}_t^* - \mathbf{w}_{n_t}\|_2 \leq l(p_{n_t}^*) \quad \forall t \in \mathcal{N}. \quad (28g)$$

We can equivalently write (28a) as

$$\begin{aligned} \frac{\partial L(p_1^*, \dots, p_N^*; \mathbf{q}_1^*, \dots, \mathbf{q}_N^*)}{\partial p_n^*} + \lambda_n - \mu_n \\ - \xi_{t_n} l'(p_n^*) = 0. \end{aligned} \quad (29)$$

Notice that  $p_n^* \neq 0$ , then according to (28d) we have  $\mu_n = 0 \ \forall n \in \mathcal{N}$ . In addition, according to (28c), we have that either  $\lambda_n = 0$  or  $p_n^* = \tilde{P}^{\max}$ . According to (28e), we have that either  $\xi_{t_n} = 0$  or  $\|\mathbf{q}_{t_n}^* - \mathbf{w}_n\|_2 - l(p_n^*) = 0$ . Since the first term of (29) is less than zero and  $l'(p_n^*) < 0$ , there must be either  $\lambda_n > 0$  or  $\xi_{t_n} > 0$ , which means that either  $p_n^* = \tilde{P}^{\max}$  or  $\|\mathbf{q}_{t_n}^* - \mathbf{w}_n\|_2 - l(p_n^*) = 0$ .

By noting that  $l(p_n)$  is a decreasing function of  $p_n$ , we know that if  $\|\mathbf{q}_n^* - \mathbf{w}_n\|_2 < l(\tilde{P}^{\max})$ , then  $p_n^* = \tilde{P}^{\max}$ ; if  $l(P^{\max}) \leq \|\mathbf{q}_{t_n}^* - \mathbf{w}_n\|_2 \leq l(0)$ , then  $p_n^*$  is the unique solution that satisfies  $\|\mathbf{q}_{t_n}^* - \mathbf{w}_n\|_2 = l(p_n^*)$ . The lemma is proved. ■

By using Lemma 1, we can simplify Problem (19) into a  $\mathbf{Q}$  optimization problem as follows:

$$\begin{aligned} \min_{\mathbf{Q}} \quad & \frac{P^F}{V} \sum_{t=0}^N \|\mathbf{q}_{t+1} - \mathbf{q}_t\|_2 + \frac{P^H D}{B} \\ & \times \sum_{t=1}^N \left[ \log_2 \left( 1 + \frac{\beta_0 \min\{l^{-1}(\|\mathbf{q}_t - \mathbf{w}_{n_t}\|_2), \tilde{P}^{\max}\}}{\sigma^2(\|\mathbf{q}_t - \mathbf{w}_{n_t}\|_2^2 + H^2)} \right) \right]^{-1} \end{aligned} \quad (30a)$$

$$\text{s.t. } \|\mathbf{q}_t - \mathbf{w}_{n_t}\|_2 \leq l_0 \quad \forall t \in \mathcal{N} \quad (30b)$$

where  $l_0 = \sqrt{(\beta_0 E_0 B / \sigma^2 D \ln 2) - H^2}$  is given by computing the limit  $l_0 = \lim_{p \rightarrow 0} l(p)$ .

The derived  $\mathbf{Q}$  optimization problem (30) can be further simplified into the more tractable one by approximating the objective function as in the following lemma.

*Lemma 2:* The following function:

$$\log_2^{-1} \left( 1 + \frac{\beta_0 \min\{l^{-1}(\|\mathbf{q}_t - \mathbf{w}_{n_t}\|_2), \tilde{P}^{\max}\}}{\sigma^2(\|\mathbf{q}_t - \mathbf{w}_{n_t}\|_2^2 + H^2)} \right) \quad (31)$$

can be approximated as

$$g(y_t(\mathbf{q}_t)) = \log_2^{-1} \left( \frac{y_t(\mathbf{q}_t) - \ln y_t(\mathbf{q}_t) + \ln(y_t(\mathbf{q}_t) - \ln y_t(\mathbf{q}_t))}{y_t(\mathbf{q}_t)} \right) \quad (32)$$

where

$$y_t(\mathbf{q}_t) \triangleq \frac{\sigma^2 D \ln 2}{\beta_0 E_0 B} \left( \|\mathbf{q}_t - \mathbf{w}_{n_t}\|_2^2 + H^2 \right). \quad (33)$$

*Proof:* First, note that in most common wireless sensor network scenarios, the value of  $p^{(1)}$  is much smaller than that of  $P^{\max}$ , therefore we have  $\tilde{P}^{\max} = p^{(1)}$  in most cases. Since by definition,  $l(p^{(1)}) = 0$ , it always holds that  $l^{-1}(\|\mathbf{q}_t - \mathbf{w}_{n_t}\|_2) \leq p^{(1)}$ , therefore (31) can be approximated by

$$\log_2^{-1} \left( 1 + \frac{\beta_0 l^{-1}(\|\mathbf{q}_t - \mathbf{w}_{n_t}\|_2)}{\sigma^2(\|\mathbf{q}_t - \mathbf{w}_{n_t}\|_2^2 + H^2)} \right). \quad (34)$$

Second, utilizing the definition of  $y_t(\mathbf{q}_t)$  in (33),  $l^{-1}(\|\mathbf{q}_t - \mathbf{w}_{n_t}\|_2)$  can be solved as

$$\begin{aligned} l^{-1}(\|\mathbf{q}_t - \mathbf{w}_{n_t}\|_2) \\ = -\frac{E_0 B W_{-1}(-ye^{-y})}{D \ln 2} - \frac{\sigma^2}{\beta_0} (\|\mathbf{q}_t - \mathbf{w}_{n_t}\|_2^2 + H^2) \end{aligned} \quad (35)$$

where  $y = y_t(\mathbf{q}_t)$ , and for notational convenience we do not distinguish between  $y$  and  $y_t(\mathbf{q}_t)$  in the following. Therefore, (34) can be written as

$$\begin{aligned} \log_2^{-1} \left( -\frac{\beta_0 E_0 B W_{-1}(-ye^{-y})}{\sigma^2 D \ln 2 (\|\mathbf{q}_t - \mathbf{w}_{n_t}\|_2^2 + H^2)} \right) \\ = \log_2^{-1} \left( -\frac{W_{-1}(-ye^{-y})}{y} \right). \end{aligned} \quad (36)$$

According to the properties of  $W_{-1}(\cdot)$ , the following approximation holds:

$$W_{-1}(x) \approx \ln(-x) - \ln(-\ln(-x)) \quad (37)$$

when  $x \rightarrow 0$ . Then, (36) can be approximated as

$$\log_2^{-1} \left( -\frac{W_{-1}(-ye^{-y})}{y} \right) \approx \log_2^{-1} \left( \frac{y - \ln y + \ln(y - \ln y)}{y} \right). \quad (38)$$

■

By utilizing Lemma 2 and introducing complementary variable  $\xi$ , problem (30) is now approximated as the following problem:

$$\min_{\mathbf{Q}, \xi} \xi \quad (39a)$$

$$\text{s.t. } \frac{P^F}{V} \sum_{t=0}^N \|\mathbf{q}_{t+1} - \mathbf{q}_t\|_2 + \frac{P^H D}{B} \sum_{t=1}^N g(y_t(\mathbf{q}_t)) - \xi \leq 0 \quad (39b)$$

$$0 \leq \|\mathbf{q}_t - \mathbf{w}_{n_t}\|_2 \leq l_0 \quad \forall t \in \mathcal{N}. \quad (39c)$$

Problem (39) can be solved by the SCA method as introduced in the previous section. However, the function  $g(y_t(\mathbf{q}_t))$  no longer has the concave characteristics as  $f_{n_t}(\mathbf{q}_t)$ , so finding a suitable convex approximating function for  $g(y_t(\mathbf{q}_t))$  requires some effort. Note that  $g(y)$  is a first-concave-then-convex function, with the critical point  $y_0 \triangleq \arg_y g''(y) = 0$ , we have the following cases for the solution to Problem (39).

- 1) Since  $y_t(\mathbf{q}_t) \geq [(\sigma^2 D \ln 2 H^2) / (\beta_0 E_0 B)] \triangleq y_1$ , if  $y_1 \geq y_0$ , then Problem (39) becomes a convex optimization problem, which can be optimally solved by the CVX toolbox.
- 2) If  $y_1 < y_0$ , we utilize the SCA method to approximate  $g(y_t(\mathbf{q}_t))$  by  $\tilde{g}_t(\mathbf{q}_t^{[k]}, \mathbf{q}_t)$  at each optimized point  $\mathbf{q}_t^{[k]}$  in the previous iteration, and solve the following problem to obtain  $\mathbf{q}_t^{[k+1]}$ :

$$\min_{\mathbf{Q}, \xi} \xi \quad (40a)$$

$$\begin{aligned} \text{s.t. } & \frac{P^F}{V} \sum_{t=0}^N \|\mathbf{q}_{t+1} - \mathbf{q}_t\|_2 - \xi \\ & + \frac{P^H D}{B} \sum_{t=1}^N \tilde{g}_t(\mathbf{q}_t^{[k]}, \mathbf{q}_t) \leq 0 \end{aligned} \quad (40b)$$

$$0 \leq \|\mathbf{q}_t - \mathbf{w}_{n_t}\|_2 \leq l_0 \quad \forall t \in \mathcal{N}. \quad (40c)$$

Problem (40) is a convex optimization problem that can be efficiently solved by the CVX toolbox. Repeatedly solving Problem (40) until convergence, the locally optimal solution to Problem (39) is derived. The expression of  $\tilde{g}_t(\mathbf{q}_t^{[k]}, \mathbf{q}_t)$  has the following two cases according to  $\mathbf{q}_t^{[k]}$ .

- a) If  $y_t(\mathbf{q}_t^{[k]}) \geq y_0$ , then

$$\tilde{g}_t(\mathbf{q}_t^{[k]}, \mathbf{q}_t) = \begin{cases} g'(y_t(\mathbf{q}_t^{[k]})) (y_t(\mathbf{q}_t) - y_t(\mathbf{q}_t^{[k]})) + g(y_t(\mathbf{q}_t^{[k]})) \\ \forall 0 \leq y_t(\mathbf{q}_t) < y_t(\mathbf{q}_t^{[k]}) \\ g(y_t(\mathbf{q}_t)) \forall y_t(\mathbf{q}_t) \geq y_t(\mathbf{q}_t^{[k]}). \end{cases} \quad (41)$$

**Algorithm 3** AQSCA Algorithm for Optimizing  $\mathbf{P}, \mathbf{Q}$ 

- 1: calculate  $y_1 = \frac{\sigma^2 D \ln 2H^2}{\beta_0 E_0 B}$ .
- 2: **if**  $y_1 \geq y_0$  **then**
- 3:     Solve (39) by the CVX toolbox.
- 4: **else**
- 5:     Initialize  $\mathbf{Q}^{[0]}$ .
- 6:     **repeat**
- 7:         Substitute  $\mathbf{q}_t^{[k]}$  into (41) if  $y_t(\mathbf{q}_t^{[k]}) \geq y_0$  and (42) if  $y_t^{[k]} < y_0$ , and solve (40) using the CVX toolbox to update  $\mathbf{Q}^{[k+1]}$ .
- 8:     **until**  $\mathbf{Q}^{[k]}$  converges
- 9: Obtain the optimal transmission power according to Lemma 1.
- 10: Output the optimization result:  $\mathbf{P}^*, \mathbf{Q}^*$ .

b) If  $y_t(\mathbf{q}_t^{[k]}) < y_0$ , then  $g(y)$  can be approximated by the following continuous differentiable function:

$$\tilde{g}_t(\mathbf{q}_t^{[k]}, \mathbf{q}_t) = \begin{cases} g'(y_t(\mathbf{q}_t^{[k]})) (y_t(\mathbf{q}_t) - y_t(\mathbf{q}_t^{[k]})) + g(y_t(\mathbf{q}_t^{[k]})) \\ \forall 0 \leq y_t(\mathbf{q}_t) < y_t(\mathbf{q}_t^{[k]}) \\ g(y_t(\mathbf{q}_t)) + \frac{g''(y_t(\mathbf{q}_t^{[k]}))}{2} (y_t(\mathbf{q}_t) - y_t(\mathbf{q}_t^{[k]}))^2 \\ \forall y_t(\mathbf{q}_t) \geq y_t(\mathbf{q}_t^{[k]}). \end{cases} \quad (42)$$

It can be easily proved that  $\tilde{g}_t(\mathbf{q}_t^{[k]}, \mathbf{q}_t)$  satisfies all the three conditions for applying the SCA method.

The above approximation method to solve Problem (19) is named as the “AQSCA algorithm.” The overall procedure of this algorithm is summarized in Algorithm 3.

**C. Complexity Analysis**

Since the Cutting-Plane method is an exact solution method for the TSP problem, which does not have theoretical justification for the complexity bounds (which in fact, may require even worse than exponential complexity), but is proved to work very successfully in most practical problems with limited computing time, we omit the worst-case computational bounds for this algorithm here. For the PSPSCA algorithm, the computational complexity is bounded by  $O((Q_1 + Q_2 + Q_3)LN^3)$ , where  $Q_1$ ,  $Q_2$ , and  $Q_3$  are the steps for the objective function evaluations at the primary and secondary bisection points and polling points of the pattern search algorithm,  $L$  is the number of iterations of the SCA algorithm [15], [25]. For the AQSCA algorithm, the computational complexity is  $O(LN^3)$ .

**V. SIMULATION RESULTS****A. Simulation Parameters**

In the simulations, the height of the UAV is set to be 100 m, the power constraint of each sensor is 25 dBm, the energy constraint of each sensor is 0.2 J, the noise power is  $-110$  dBm, the bandwidth is 1 MHz, the data size of each sensor’s data packet is 6 Mbits, the hovering power of the UAV is 168.4842 W, the flying power of the UAV is 161.5225 W, the flying speed of the UAV is 18.2951 m/s [26]. The related system parameters are summarized in Table I.

TABLE I  
SIMULATION PARAMETERS

Parameter	Value
Number of sensors	20
Sensor distribution area	1000 m $\times$ 1000 m
UAV altitude $H$	100 m
Sensor maximum transmit power $P^{\max}$	25 dBm
Sensor energy budget $E_0$	0.2 J
AWGN noise power $\sigma^2$	-110 dBm
System bandwidth $B$	1 MHz
Channel power gain at unit distance $\beta_0$	$10^{-6}$
Sensor data size $D$	20 Mbits
UAV flying power $P^F$	161.5225 W
UAV hovering power $P^H$	168.4842 W
UAV flying speed $V$	18.2951 m/s

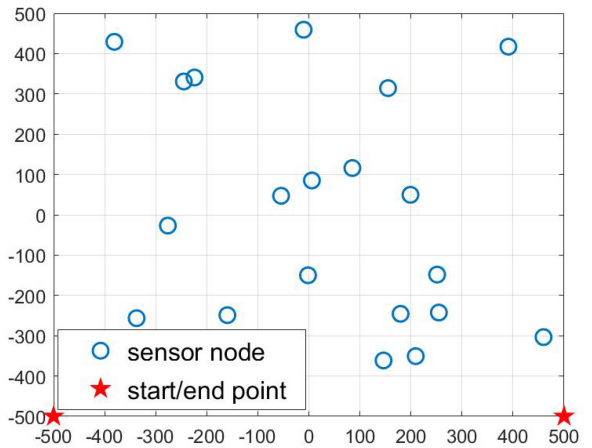


Fig. 2. Sensor positions and the start and endpoints of the UAV trajectory.

If not specified, the sensor positions and the start and endpoints of the trajectory are given in Fig. 2.

**B. Comparison of Different  $\mathbf{P}, \mathbf{Q}$  Optimizing Algorithms**

First, we compare different schemes for solving  $\mathbf{P}, \mathbf{Q}$ . Four schemes are compared, namely, the PSPSCA algorithm, the AQSCA algorithm, a simplified version of the PSPSCA algorithm where the pattern search method is applied to each  $p_u$  sequentially (termed as “sequential pattern search” in the figures), and the traditional method of alternately optimizing  $\mathbf{P}$  and  $\mathbf{Q}$  until convergence (termed as “alternate  $\mathbf{P}, \mathbf{Q}$ ” in the figures). All the above-mentioned algorithms adopt the Cutting-Plane method for optimizing  $\mathbf{A}$ .

In Fig. 3, four algorithms are compared under the energy constraint of  $E_0 = 0.2$  J. It is seen from this figure that the AQSCA algorithm performs as well as the PSPSCA and the sequential pattern search of  $\mathbf{P}$ , while the alternate optimization of  $\mathbf{P}$  and  $\mathbf{Q}$  gives much worse result. The reason that the alternate optimization of  $\mathbf{P}$  and  $\mathbf{Q}$  fails to provide satisfactory performance is that, each time when  $\mathbf{P}$  is optimized, the feasible search region for  $\mathbf{Q}$  shrinks, hence the  $\mathbf{Q}$  optimization will be restricted within a smaller and smaller region. Therefore, the optimal trajectories which deviate far from the sensor nodes are missed by the alternate  $\mathbf{P}, \mathbf{Q}$  algorithm.

For the best-performing AQSCA algorithm, PSPSCA algorithm, and the sequential pattern search algorithm, we compare

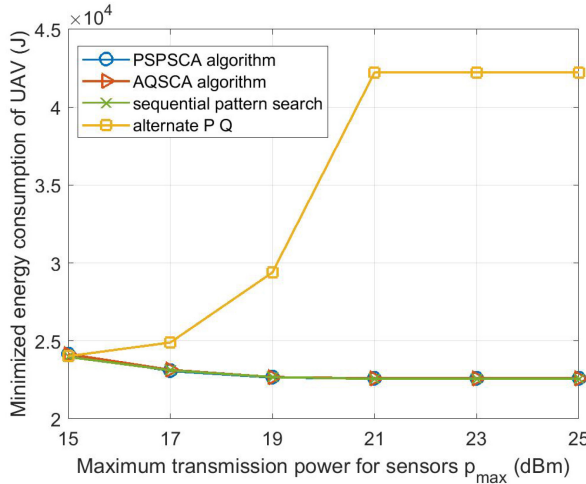


Fig. 3. Comparison of the minimized UAV energy consumption Verses the maximum transmission power of sensors under four  $P, Q$  optimizing algorithms, with  $E_0 = 0.2$  J.

TABLE II  
PROCESSING TIMES OF THREE ALGORITHMS (IN SECONDS)

	15 dBm	17 dBm	19 dBm
AQSCA algorithm	27.7014	27.1998	23.8580
PSPSCA algorithm	110.0013	$2.6589 \times 10^3$	$2.6548 \times 10^3$
Sequential pattern search	658.4714	$2.3214 \times 10^3$	$1.3340 \times 10^3$
21 dBm	26.2842	26.6149	26.5604
AQSCA algorithm	4.9239 $\times 10^3$	$4.9236 \times 10^3$	$5.3574 \times 10^3$
PSPSCA algorithm	4.6997 $\times 10^3$	$4.9549 \times 10^3$	$4.7295 \times 10^3$

their processing time. The processing time of these three algorithms are listed in Table II.

It is obvious from Table II that the AQSCA algorithm requires much less processing time than the other two benchmark schemes. In practice, the sequential pattern search of  $P$  and the pattern search of  $P$  requires prohibitively high processing time even for a small number of sensors (in this case 20 sensors). Therefore, the AQSCA algorithm exhibits superiority in both performance and processing time.

In Fig. 4, four algorithms are compared under a larger energy constraint  $E_0 = 0.5$  J. It is shown that the alternate  $P, Q$  algorithm exhibits good performance when  $P^{\max}$  is small. This can be explained by the fact that under a larger energy budget,  $E_0 = 0.5$  J, the feasible region is larger. Although the alternate optimization of  $P$  and  $Q$  shrinks the feasible search region, the smallest search region still covers the optimal trajectory, therefore making no influence on the result produced by the alternate  $P, Q$  algorithm. However, this phenomenon disappears when the power budget increases. Therefore, we can conclude that the most suitable  $P, Q$  optimization algorithm is the AQSCA algorithm, with both good performance and little computation time.

To further analyze the performance of the AQSCA algorithm, we compare it with the PSPSCA algorithm under different sensor distributions, with both identical and different start and endpoints, to test the robustness of the AQSCA algorithm. In particular, we consider three sensor distribution cases.

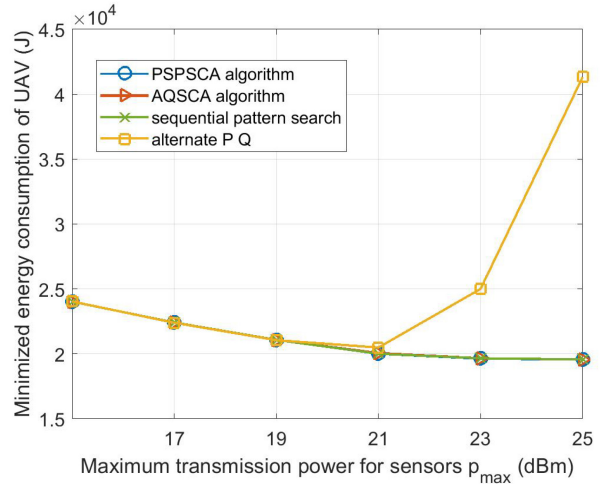


Fig. 4. Comparison of the minimized UAV energy consumption Verses the maximum transmission power of sensors under four  $P, Q$  optimizing algorithms, with  $E_0 = 0.5$  J.

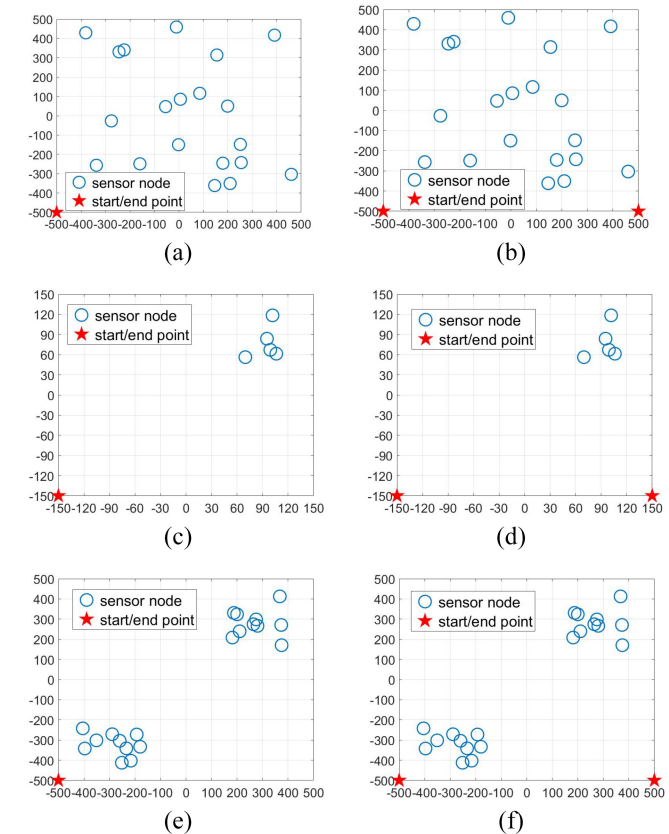


Fig. 5. Three typical sensor distributions with identical and different start/endpoints. (a) Case 1, identical start/endpoints (b) Case 1, different start/endpoints (c) Case 2, identical start/endpoints (d) Case 2, different start/endpoints (e) Case 3, identical start/endpoints (f) Case 3, different start/endpoints.

*Case 1:* 20 sensors are uniformly distributed in the given area.

*Case 2:* Five sensors form a group on the upper-right corner of a smaller area (150 m  $\times$  150 m).

*Case 3:* 20 sensors form two groups on the upper-right and lower-left corners of the given area.

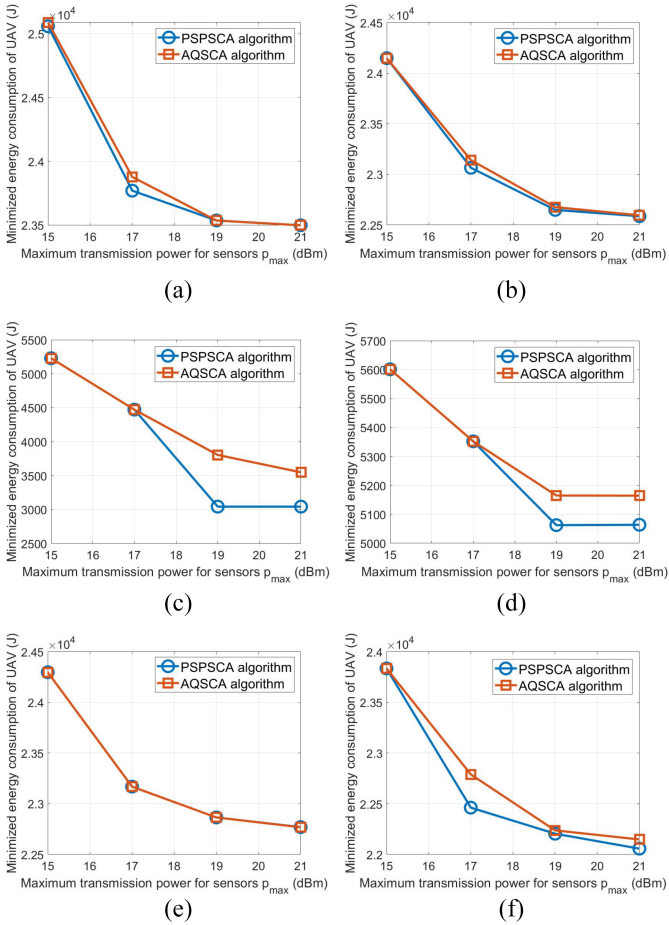


Fig. 6. Minimized UAV energy consumption optimized by the AQSCA algorithm and the PSPSCA algorithm under sensor distribution scenarios given in Fig. 5. (a) Case 1, identical start/endpoints. (b) Case 1, different start/endpoints. (c) Case 2, identical start/endpoints. (d) Case 2, different start/endpoints. (e) Case 3, identical start/endpoints. (f) Case 3, different start/endpoints.

The sensor positions of the above three cases are depicted in Fig. 5.

The comparison of the AQSCA and PSPSCA algorithms under three sensor distribution cases with both identical and different start/endpoints are plotted in Fig. 6. The result of the AQSCA algorithm is compared with the PSPSCA algorithm to see how much performance gap is there under different sensor distributions. It can be seen from the figure that the AQSCA algorithm achieves nearly the same performance as the PSPSCA algorithm when there are a large number of sensors (e.g., 20 sensors in cases 1 and 3). When the number of sensors is small (e.g., five sensors in case 2), the AQSCA algorithm performs well at small  $P^{\max}$ 's, but becomes inferior at larger  $P^{\max}$ 's. This may be because when the number of sensors is small, the AQSCA algorithm is more likely to be trapped in a local optimum, which is far from the globally optimal solution. Still, the gaps between the two algorithms, even when the number of sensors is small, are within the acceptable region. In addition, the AQSCA has more advantage in reducing the computational time when the number of sensors is larger, and fortunately, it performs fairly

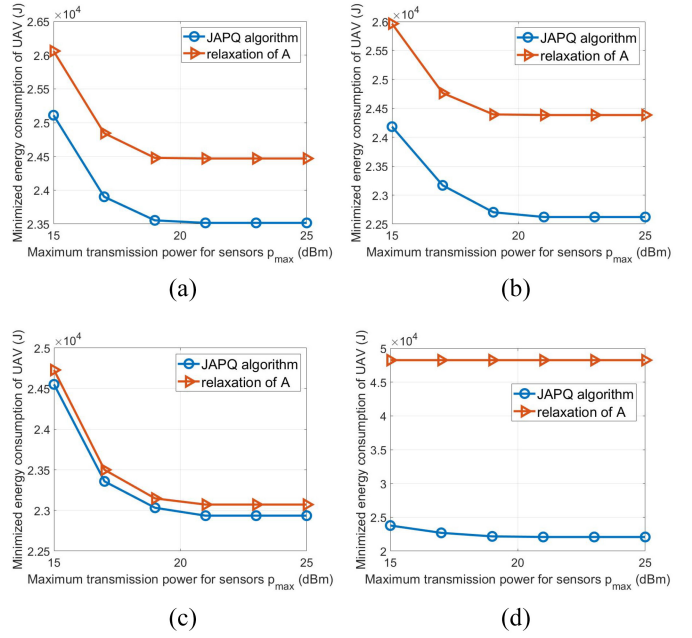


Fig. 7. Minimized UAV energy consumption of the JAPQ algorithm and the relaxation of  $A$  algorithm under distribution scenarios given in Fig. 5. (a) Case 1, identical start/endpoints. (b) Case 1, different start/endpoints. (c) Case 3, identical start/endpoints. (d) Case 3, different start/endpoints.

well under this circumstance. Therefore, we can conclude that the AQSCA algorithm achieves close performance to the PSPSCA algorithm, at a small cost of performance when  $N$  is small, and with largely reduced computational time. In particular, the AQSCA algorithm is most suitable to be adopted when the number of sensors is large, with both near-optimal performance and greatly reduced computational time.

### C. Comparison of Different $A$ Optimizing Algorithms

Next, we compare different algorithms for optimizing  $A$ . The Cutting-Plane method is compared with a benchmark scheme: the widely used “relaxation of  $A$ ” algorithm. The idea of the relaxation of  $A$  algorithm is that, the integer variable  $A$  is relaxed into continuous variables, and the  $A$  optimization problem is solved by continuous-variable optimization techniques, and finally the continuous solutions are rounded into integer values. For a fair comparison, both of the algorithms use the AQSCA algorithm for  $P, Q$  optimization. The comparison of the two algorithms under different scenarios are presented in Fig. 7.

It can be seen that the Cutting-Plane method generally outperforms the relaxation of  $A$  algorithm in every considered case. In some cases, the gap between the two algorithms are evident; while in others, the gap is relatively small. What can be concluded from the results is that, the relaxation of  $A$  algorithm leads to some performance loss due to the relaxation and rounding process, while the effect of the process vary according to different sensor distribution scenarios. Since the Cutting-Plane method is proved to be an efficient TSP solution algorithm in most practical cases, which can also be inferred from the running time given in Table II, it is advantageous to use the Cutting-Plane method for  $A$  optimization.

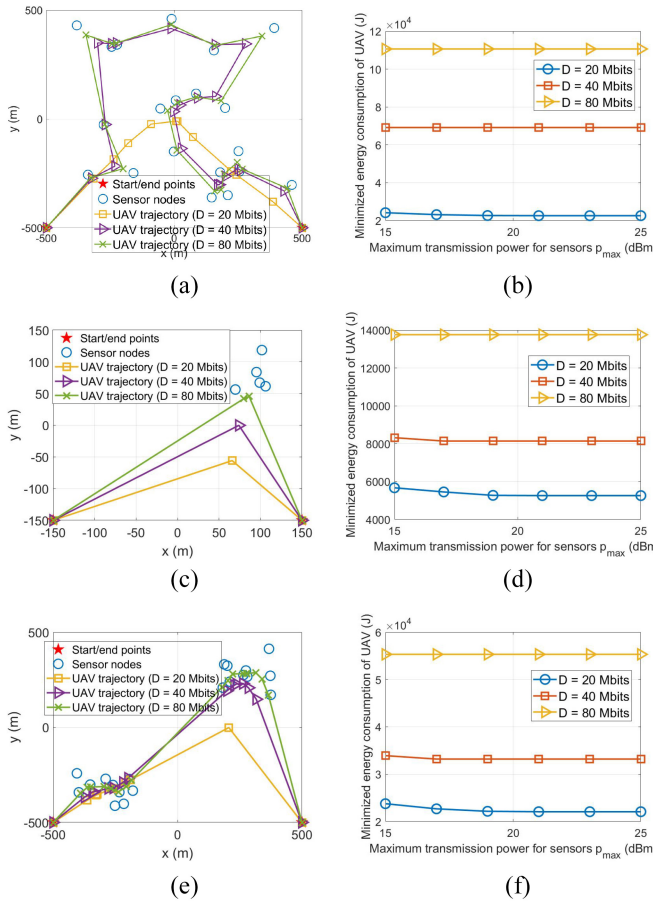


Fig. 8. Trajectory and minimized energy consumption of the UAV under three different  $D$ s under different distribution scenarios. (a) Case 1, trajectory. (b) Case 1, optimized energy consumption. (c) Case 2, trajectory. (d) Case 2, optimized energy consumption. (e) Case 3, trajectory. (f) Case 3, optimized energy consumption.

#### D. Effect of System Parameters on Performance

Finally, we analyze the effect of several system parameters on the minimized UAV energy consumption, as well as on the optimized trajectory.

In Fig. 8, the optimized UAV trajectory as well as its energy consumption versus sensors' power limit  $P^{max}$  under different sensor data size  $D$ s are plotted. It can be seen from the figure that as  $D$  increases, the UAV flies closer to the sensor nodes for data collection. This reason is two fold. First, a larger data size leads to a larger uploading energy consumption of the sensors, to meet the energy budget of each sensor, the UAV has to fly closer to the sensors to reduce the uploading energy. Second, the data size  $D$  also influences the hovering energy of the UAV. When  $D$  increases, the hovering time increases as well, hence the hovering energy takes a larger part in the overall energy consumption of the UAV. To reduce the hovering energy consumption, the UAV also tends to fly closer to the sensors. For the energy consumption, larger  $D$  leads to larger UAV energy consumption, which is evident since the hovering time increases with  $D$ .

In Fig. 9, the optimized UAV trajectory as well as the energy consumption versus sensors' power limit  $P^{max}$  under different sensor energy budget  $E_0$ s are plotted. It can be observed that

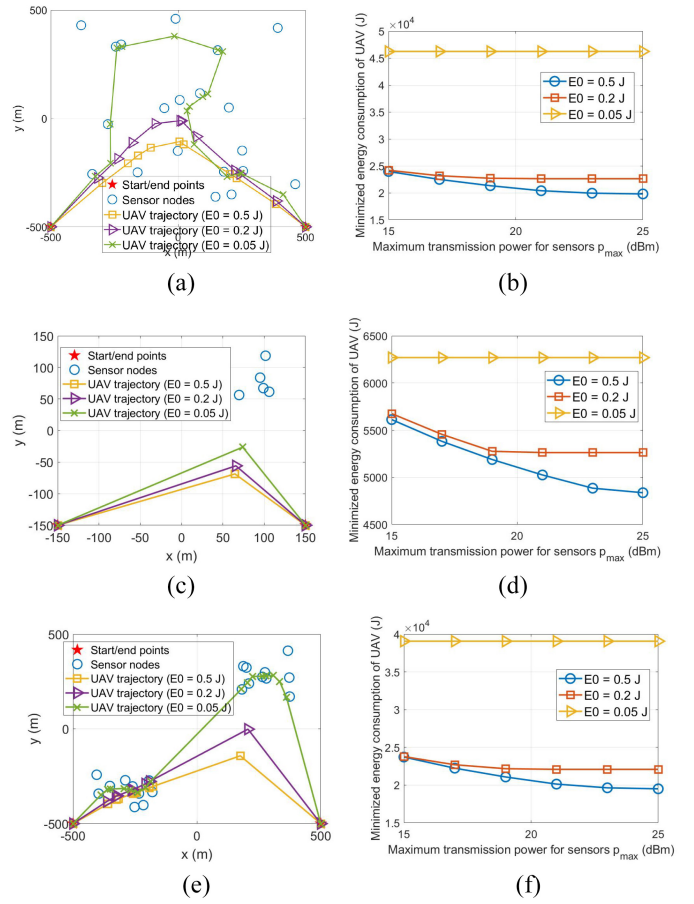


Fig. 9. Trajectory and minimized energy consumption of the UAV under three different  $E_0$ s under different distribution scenarios. (a) Case 1, trajectory. (b) Case 1, optimized energy consumption. (c) Case 2, trajectory. (d) Case 2, optimized energy consumption. (e) Case 3, trajectory. (f) Case 3, optimized energy consumption.

the UAV also flies closer to the sensors as  $E_0$  decreases. This can be similarly explained that a smaller  $E_0$  means a smaller sensor energy budget, and to meet this shrinking energy budget the UAV has to fly closer to the sensors to reduce the sensor uploading energy consumption. Another interesting observation can be made from comparing the minimized UAV energy consumption results with Fig. 8. If we look at the expression of  $l(p_{n_i})$ , we can observe that the increase of  $D$  or the decrease of  $E_0$  all leads to the decrease in  $l(p_{n_i})$ , which defines the feasible flying region of the UAV. However, when we increase  $D$  or decrease  $E_0$  to make the same extent of decrease in  $l(p_{n_i})$ , the UAV energy consumption is increased more significantly in Fig. 8. This can be explained by the fact that  $D$  not only influences the feasible region parameter  $l(p_{n_i})$ , but also the objective function. Therefore, with the same extent of increase/decrease, the increase of  $D$  not only shrinks the feasible region, but also increases the hovering energy consumption, leading to a larger influence on the minimized UAV energy consumption.

## VI. CONCLUSION

In this article, we have studied the joint optimization problem of UAV's trajectory and sensors' uploading power

for the UAV-assisted sensor networks, aiming at minimizing the energy consumption of the UAV. The problem has been solved by iteratively computing the serving orders for sensors, and UAV hovering positions and sensor uploading power. The serving orders for sensors is computed by the Cutting-Plane method, while the UAV hovering positions and sensor uploading power optimization is proposed to be solved by two algorithms: 1) the optimal PSPSCA algorithm and 2) the low-complexity AQSCA algorithm. For the AQSCA algorithm, a closed-form expression of optimal transmit power has been derived as a function with respect to the hovering positions of the UAV. In the simulation results, we have revealed that the Cutting-Plane algorithm for the serving order optimization, and the AQSCA algorithm for the hovering position and uploading power optimization, outperforms other benchmark schemes under most user distributions, especially when there are a large number of sensors. In addition, the effect of system parameters (e.g., the energy budget  $E_0$  and the data size  $D$  of sensors) on the optimized trajectory has been analyzed. It has been found that as  $D$  increases or  $E_0$  decreases, the UAV flies closer to the sensor nodes, while the effect of  $D$  is more significant.

## REFERENCES

- [1] D. Kim, R. N. Uma, B. H. Abay, W. Wu, W. Wang, and A. O. Tokuta, "Minimum latency multiple data MULE trajectory planning in wireless sensor networks," *IEEE Trans. Mobile Comput.*, vol. 13, no. 4, pp. 838–851, Apr. 2014.
- [2] R. Sugihara and R. K. Gupta, "Optimal speed control of mobile node for data collection in sensor networks," *IEEE Trans. Mobile Comput.*, vol. 9, no. 1, pp. 127–139, Jan. 2010.
- [3] B. Yuan, M. Orlowska, and S. Sadiq, "On the optimal robot routing problem in wireless sensor networks," *IEEE Trans. Knowl. Data Eng.*, vol. 19, no. 9, pp. 1252–1261, Sep. 2007.
- [4] J. Baek, S. I. Han, and Y. Han, "Energy-efficient UAV routing for wireless sensor networks," *IEEE Trans. Veh. Technol.*, vol. 69, no. 2, pp. 1741–1750, Feb. 2020.
- [5] M. Samir, S. Sharafeddine, C. M. Assi, T. M. Nguyen, and A. Ghrayeb, "UAV trajectory planning for data collection from time-constrained IoT devices," *IEEE Trans. Wireless Commun.*, vol. 19, no. 1, pp. 34–46, Jan. 2020.
- [6] J. Li *et al.*, "Joint optimization on trajectory, altitude, velocity, and link scheduling for minimum mission time in UAV-aided data collection," *IEEE Internet Things J.*, vol. 7, no. 2, pp. 1464–1475, Feb. 2020.
- [7] Y. Zeng and R. Zhang, "Energy-efficient UAV communication with trajectory optimization," *IEEE Trans. Wireless Commun.*, vol. 16, no. 6, pp. 3747–3760, Jun. 2017.
- [8] C. Zhan and H. Lai, "Energy minimization in Internet-of-Things system based on rotary-wing UAV," *IEEE Wireless Commun. Lett.*, vol. 8, no. 5, pp. 1341–1344, Oct. 2019.
- [9] D. Ebrahimi, S. Sharafeddine, P. H. Ho, and C. Assi, "UAV-aided projection-based compressive data gathering in wireless sensor networks," *IEEE Internet Things J.*, vol. 6, no. 2, pp. 1893–1905, Apr. 2019.
- [10] C. Zhan and Y. Zeng, "Aerial-ground cost tradeoff for multi-UAV-enabled data collection in wireless sensor networks," *IEEE Trans. Commun.*, vol. 68, no. 3, pp. 1937–1950, Mar. 2020.
- [11] C. Zhan, Y. Zeng, and R. Zhang, "Energy-efficient data collection in UAV enabled wireless sensor network," *IEEE Wireless Commun. Lett.*, vol. 7, no. 3, pp. 328–331, Jun. 2018.
- [12] C. You and R. Zhang, "Hybrid offline-online design for UAV-enabled data harvesting in probabilistic LoS channels," *IEEE Trans. Wireless Commun.*, vol. 19, no. 6, pp. 3753–3768, Jun. 2020.
- [13] C. Shen, T. H. Chang, J. Gong, Y. Zeng, and R. Zhang, "Multi-UAV interference coordination via joint trajectory and power control," *IEEE Trans. Signal Process.*, vol. 68, pp. 843–858, Jan. 2020.
- [14] J. Gong, T. H. Chang, C. Shen, and X. Chen, "Flight time minimization of UAV for data collection over wireless sensor networks," *IEEE J. Sel. Areas Commun.*, vol. 36, no. 9, pp. 1942–1954, Sep. 2018.
- [15] C. Zhan and Y. Zeng, "Completion time minimization for multi-UAV-enabled data collection," *IEEE Trans. Wireless Commun.*, vol. 18, no. 10, pp. 4859–4872, Oct. 2019.
- [16] J. Liu, P. Tong, X. Wang, B. Bai, and H. Dai, "UAV-aided data collection for information freshness in wireless sensor networks," *IEEE Trans. Wireless Commun.*, vol. 20, no. 4, pp. 2368–2382, Apr. 2021.
- [17] M. Chen, W. Liang, and S. K. Das, "Data collection utility maximization in wireless sensor networks via efficient determination of UAV hovering locations," in *Proc. IEEE Int. Conf. Pervasive Comput. Commun. (PerCom)*, 2021, pp. 1–10.
- [18] W. Chen, S. Zhao, R. Zhang, Y. Chen, and L. Yang, "UAV-assisted data collection with nonorthogonal multiple access," *IEEE Internet Things J.*, vol. 8, no. 1, pp. 501–511, Jan. 2021.
- [19] M. Chen, W. Liang, and J. Li, "Energy-efficient data collection maximization for UAV-assisted wireless sensor networks," in *Proc. IEEE Wireless Commun. Netw. Conf. (WCNC)*, 2021, pp. 1–7.
- [20] H. Hu, K. Xiong, G. Qu, Q. Ni, P. Fan, and K. Ben Letaief, "AoI-minimal trajectory planning and data collection in UAV-assisted wireless powered IoT networks," *IEEE Internet Things J.*, vol. 8, no. 2, pp. 1211–1223, Jan. 2021.
- [21] Y. Li *et al.*, "Data collection maximization in IoT-sensor networks via an energy-constrained UAV," *IEEE Trans. Mobile Comput.*, early access, May 31, 2021, doi: [10.1109/TMC.2021.3084972](https://doi.org/10.1109/TMC.2021.3084972).
- [22] T. Feng, L. Xie, J. Yao, and J. Xu, "UAV-enabled data collection for wireless sensor networks with distributed beamforming," *IEEE Trans. Wireless Commun.*, early access, Aug. 17, 2021, doi: [10.1109/TWC.2021.3103739](https://doi.org/10.1109/TWC.2021.3103739).
- [23] G. Reinelt, *The Traveling Salesman: Computational Solutions for TSP Applications* (Lecture Notes in Computer Science), vol. 840. Heidelberg, Germany: Springer-Verlag, 1994. [Online]. Available: <https://search.ebscohost.com/login.aspx?direct=true&db=cat05354a&AN=seul.00000843019&lang=zh-cn&site=eds-live>
- [24] M. Chiang, C. W. Tan, D. P. Palomar, D. O'Neill, and D. Julian, "Power control by geometric programming," *IEEE Trans. Wireless Commun.*, vol. 6, no. 7, pp. 2640–2650, Jul. 2007.
- [25] M. Jasim and N. Ghani, "Generalized pattern search for beam discovery in millimeter wave systems," in *Proc. IEEE 86th Veh. Technol. Conf. (VTC-Fall)*, 2017, pp. 1–5.
- [26] Y. Zeng, J. Xu, and R. Zhang, "Energy minimization for wireless communication with rotary-wing UAV," *IEEE Trans. Wireless Commun.*, vol. 18, no. 4, pp. 2329–2345, Apr. 2019. [Online]. Available: <https://ieeexplore.ieee.org/document/8663615/>



**Yinlu Wang** (Student Member, IEEE) received the B.S. degree in opto-electronic science and technology from Nankai University, Tianjin, China, in 2015. She is currently pursuing the Ph.D. degree with the National Mobile Communications Research Laboratory, Southeast University, Nanjing, China.

From September 2019 to September 2020, she has been an international visiting graduate student with the Department of Electrical and Computer Engineering, University of Waterloo, Waterloo, ON, Canada. Her research interests include mobile edge computing networks, next-generation wireless networks, D2D communication, mixed-integer programming problems, and scheduling algorithms.



**Ming Chen** (Member, IEEE) received the Ph.D. degree from Mathematics Department, Nanjing University, Nanjing, China, in 1996.

In July 1996, he joined the National Mobile Communications Research Laboratory, Southeast University, Nanjing, as a Lecturer. From 1998 to 2003, he was an Associate Professor with the National Mobile Communications Research Laboratory and where has been a Professor since 2003. He has completed more than 40 research projects in the role of director by now, among which

there are more than 15 projects are issued by national ministries, supervised more than 30 Ph.D. and 100 M.Sc. students and published more than 300 journal papers as coauthor. His research interests include baseband signal processing, radio and computing resource allocation and network planning for all generation mobile communication systems, visible light communication systems, mobile edge computing systems, and satellite mobile communications.

Prof. Chen won twice the First Level Provincial Progress Awards in Science and Technology.



**Cunhua Pan** (Member, IEEE) received the B.S. and Ph.D. degrees from the School of Information Science and Engineering, Southeast University, Nanjing, China, in 2010 and 2015, respectively.

From 2015 to 2016, he was a Research Associate with the University of Kent, Canterbury, U.K. He held a postdoctoral position with the Queen Mary University of London, London, U.K., from 2016 and 2019, where he is currently a Lecturer. His research interests mainly include reconfigurable intelligent surfaces, intelligent reflection surface, ultrareliable low latency communication, machine learning, UAV, Internet of Things, and mobile edge computing.

Dr. Pan is a Workshop Organizer in IEEE ICCC 2021 on the topic of Reconfigurable Intelligent Surfaces for Next Generation Wireless Communications (RIS for 6G Networks) and a Workshop Organizer in IEEE Globecom 2021 on the topic of Reconfigurable Intelligent Surfaces for future wireless communications. He is currently the Workshops and a Symposia Officer for Reconfigurable Intelligent Surfaces Emerging Technology Initiative. He is currently an Editor of IEEE WIRELESS COMMUNICATION LETTERS, IEEE COMMUNICATIONS LETTERS, and IEEE ACCESS. He also serves as a Leading Guest Editor for IEEE JOURNAL OF SELECTED TOPICS IN SIGNAL PROCESSING on the Special Issue on Advanced Signal Processing for Reconfigurable Intelligent Surface-Aided 6G Networks, IEEE Vehicular Technology Magazine on the special issue on Backscatter and Reconfigurable Intelligent Surface Empowered Wireless Communications in 6G, IEEE OPEN JOURNAL OF VEHICULAR TECHNOLOGY on the special issue of Reconfigurable Intelligent Surface Empowered Wireless Communications in 6G and Beyond, and IEEE ACCESS on the Special Issue on Reconfigurable Intelligent Surface Aided Communications for 6G and Beyond. He serves as the TPC Member for numerous conferences, such as ICC and GLOBECOM, and the Student Travel Grant Chair for ICC 2019.



**Kezhi Wang** (Senior Member, IEEE) received the B.E. and M.E. degrees with the School of Automation, Chongqing University, Chongqing, China, in 2008 and 2011, respectively, and the Ph.D. degree in engineering from the University of Warwick, Coventry, U.K., in 2015.

He was a Senior Research Officer with the University of Essex, Colchester, U.K. He is currently a Senior Lecturer with the Department of Computer and Information Sciences, Northumbria University Newcastle, Newcastle upon Tyne, U.K. His research interests include wireless communications and machine learning.



**Yijin Pan** (Member, IEEE) received the B.S. and M.S. degrees in communication engineering from Chongqing University, Chongqing, China, in 2011 and 2014, respectively, and the Ph.D. degree from the School of Information Science and Engineering, Southeast University, Nanjing, China, in 2018.

She visited the University of Kent, Kent, U.K., from November 2015 to November 2016. She held a Newton Fellowship with the University of Kent from March 2019 to April 2021. She is currently holds a lecture position with the National Mobile Communications Research Laboratory, Southeast University. Her current research interests include D2D content caching, nonorthogonal multiple access, and mobile edge computing.

Dr. Pan was a TPC Member of IEEE ICC from 2015 to 2019 and Globecom from 2017 to 2019.